

Direct Observation of Dijets in Central Au + Au Collisions at $\sqrt{s_{NN}} = 200$ GeV

J. Adams,² M. M. Aggarwal,²⁹ Z. Ahammed,⁴⁴ J. Amonett,¹⁹ B. D. Anderson,¹⁹ M. Anderson,⁶ D. Arkhipkin,¹² G. S. Averichev,¹¹ Y. Bai,²⁷ J. Balewski,¹⁶ O. Barannikova,³² L. S. Barnby,² J. Baudot,¹⁷ S. Bekele,²⁸ V. V. Belaga,¹¹ A. Bellingeri-Laurikainen,³⁹ R. Bellwied,⁴⁷ B. I. Bezverkhny,⁴⁹ S. Bhardwaj,³⁴ A. Bhasin,¹⁸ A. K. Bhati,²⁹ H. Bichsel,⁴⁶ J. Bielcik,⁴⁹ J. Bielcikova,⁴⁹ L. C. Bland,³ C. O. Blyth,² S-L. Blyth,²¹ B. E. Bonner,³⁵ M. Botje,²⁷ J. Bouchet,³⁹ A. V. Brandin,²⁵ A. Bravar,³ M. Bystersky,¹⁰ R. V. Cadman,¹ X. Z. Cai,³⁸ H. Caines,⁴⁹ M. Calderón de la Barca Sánchez,⁶ J. Castillo,²⁷ O. Catu,⁴⁹ D. Cebra,⁶ Z. Chajecki,²⁸ P. Chaloupka,¹⁰ S. Chattopadhyay,⁴⁴ H. F. Chen,³⁷ J. H. Chen,³⁸ Y. Chen,⁷ J. Cheng,⁴² M. Cherney,⁹ A. Chikanian,⁴⁹ H. A. Choi,³³ W. Christie,³ J. P. Coffin,¹⁷ T. M. Cormier,⁴⁷ M. R. Cosentino,³⁶ J. G. Cramer,⁴⁶ H. J. Crawford,⁵ D. Das,⁴⁴ S. Das,⁴⁴ M. Daugherty,⁴¹ M. M. de Moura,³⁶ T. G. Dedovich,¹¹ M. DePhillips,³ A. A. Derevschikov,³¹ L. Didenko,³ T. Dietel,¹³ P. Djawotho,¹⁶ S. M. Dogra,¹⁸ W. J. Dong,⁷ X. Dong,³⁷ J. E. Draper,⁶ F. Du,⁴⁹ V. B. Dunin,¹¹ J. C. Dunlop,³ M. R. Dutta Mazumdar,⁴⁴ V. Eckardt,²³ W. R. Edwards,²¹ L. G. Efimov,¹¹ V. Emelianov,²⁵ J. Engelage,⁵ G. Eppley,³⁵ B. Erazmus,³⁹ M. Estienne,¹⁷ P. Fachini,³ R. Fatemi,²² J. Fedorisin,¹¹ K. Filimonov,²¹ P. Filip,¹² E. Finch,⁴⁹ V. Fine,³ Y. Fisyak,³ J. Fu,⁴⁸ C. A. Gagliardi,⁴⁰ L. Gaillard,² J. Gans,⁴⁹ M. S. Ganti,⁴⁴ V. Ghazikhanian,⁷ P. Ghosh,⁴⁴ J. E. Gonzalez,⁷ Y. G. Gorbunov,⁹ H. Gos,⁴⁵ O. Grebenyuk,²⁷ D. Grosnick,⁴³ S. M. Guertin,⁷ K. S. F. F. Guimaraes,³⁶ Y. Guo,⁴⁷ N. Gupta,¹⁸ T. D. Gutierrez,⁶ B. Haag,⁶ T. J. Hallman,³ A. Hamed,⁴⁷ J. W. Harris,⁴⁹ W. He,¹⁶ M. Heinz,⁴⁹ T. W. Henry,⁴⁰ S. Hepplemann,³⁰ B. Hippolyte,¹⁷ A. Hirsch,³² E. Hjort,²¹ G. W. Hoffmann,⁴¹ M. J. Horner,²¹ H. Z. Huang,⁷ S. L. Huang,³⁷ E. W. Hughes,⁴ T. J. Humanic,²⁸ G. Igo,⁷ P. Jacobs,²¹ W. W. Jacobs,¹⁶ P. Jakl,¹⁰ F. Jia,²⁰ H. Jiang,⁷ P. G. Jones,² E. G. Judd,⁵ S. Kabana,³⁹ K. Kang,⁴² J. Kapitan,¹⁰ M. Kaplan,⁸ D. Keane,¹⁹ A. Kechechyan,¹¹ V. Yu. Khodyrev,³¹ B. C. Kim,³³ J. Kiryluk,²² A. Kisel,⁴⁵ E. M. Kislov,¹¹ S. R. Klein,²¹ D. D. Koetke,⁴³ T. Kollegger,¹³ M. Kopytine,¹⁹ L. Kotchenda,²⁵ V. Kouchpil,¹⁰ K. L. Kowalik,²¹ M. Kramer,²⁶ P. Kravtsov,²⁵ V. I. Kravtsov,³¹ K. Krueger,¹ C. Kuhn,¹⁷ A. I. Kulikov,¹¹ A. Kumar,²⁹ A. A. Kuznetsov,¹¹ M. A. C. Lamont,⁴⁹ J. M. Landgraf,³ S. Lange,¹³ S. LaPointe,⁴⁷ F. Laue,³ J. Lauret,³ A. Lebedev,³ R. Lednicky,¹² C-H. Lee,³³ S. Lehocka,¹¹ M. J. LeVine,³ C. Li,³⁷ Q. Li,⁴⁷ Y. Li,⁴² G. Lin,⁴⁹ S. J. Lindenbaum,²⁶ M. A. Lisa,²⁸ F. Liu,⁴⁸ H. Liu,³⁷ J. Liu,³⁵ L. Liu,⁴⁸ Z. Liu,⁴⁸ T. Ljubicic,³ W. J. Llope,³⁵ H. Long,⁷ R. S. Longacre,³ M. Lopez-Noriega,²⁸ W. A. Love,³ Y. Lu,⁴⁸ T. Ludlam,³ D. Lynn,³ G. L. Ma,³⁸ J. G. Ma,⁷ Y. G. Ma,³⁸ D. Magestro,²⁸ D. P. Mahapatra,¹⁴ R. Majka,⁴⁹ L. K. Mangotra,¹⁸ R. Manweiler,⁴³ S. Margetis,¹⁹ C. Markert,¹⁹ L. Martin,³⁹ H. S. Matis,²¹ Yu. A. Matulenko,³¹ C. J. McClain,¹ T. S. McShane,⁹ Yu. Melnick,³¹ A. Meschanin,³¹ M. L. Miller,²² N. G. Minaev,³¹ S. Mioduszewski,⁴⁰ C. Mironov,¹⁹ A. Mischke,²⁷ D. K. Mishra,¹⁴ J. Mitchell,³⁵ B. Mohanty,⁴⁴ L. Molnar,³² C. F. Moore,⁴¹ D. A. Morozov,³¹ M. G. Munhoz,³⁶ B. K. Nandi,¹⁵ C. Nattrass,⁴⁹ T. K. Nayak,⁴⁴ J. M. Nelson,² P. K. Netrakanti,⁴⁴ V. A. Nikitin,¹² L. V. Nogach,³¹ S. B. Nurushev,³¹ G. Odyniec,²¹ A. Ogawa,³ V. Okorokov,²⁵ M. Oldenburg,²¹ D. Olson,²¹ M. Pachr,¹⁰ S. K. Pal,⁴⁴ Y. Panebratsev,¹¹ S. Y. Panitkin,³ A. I. Pavlinov,⁴⁷ T. Pawlak,⁴⁵ T. Peitzmann,²⁷ V. Perevoztchikov,³ C. Perkins,⁵ W. Peryt,⁴⁵ V. A. Petrov,⁴⁷ S. C. Phatak,¹⁴ R. Picha,⁶ M. Planinic,⁵⁰ J. Pluta,⁴⁵ N. Poljak,⁵⁰ N. Porile,³² J. Porter,⁴⁶ A. M. Poskanzer,²¹ M. Potekhin,³ E. Potrebenikova,¹¹ B. V. K. S. Potukuchi,¹⁸ D. Prindle,⁴⁶ C. Pruneau,⁴⁷ J. Putschke,²¹ G. Rakness,³⁰ R. Raniwala,³⁴ S. Raniwala,³⁴ R. L. Ray,⁴¹ S. V. Razin,¹¹ J. Reinnarth,³⁹ D. Relyea,⁴ F. Retiere,²¹ A. Ridiger,²⁵ H. G. Ritter,²¹ J. B. Roberts,³⁵ O. V. Rogachevskiy,¹¹ J. L. Romero,⁶ A. Rose,²¹ C. Roy,³⁹ L. Ruan,²¹ M. J. Russcher,²⁷ R. Sahoo,¹⁴ I. Sakrejda,²¹ S. Salur,⁴⁹ J. Sandweiss,⁴⁹ M. Sarsour,⁴⁰ P. S. Sazhin,¹¹ J. Schambach,⁴¹ R. P. Scharenberg,³² N. Schmitz,²³ K. Schweda,²¹ J. Seger,⁹ I. Selyuzhenkov,⁴⁷ P. Seyboth,²³ A. Shabetai,²¹ E. Shahaliev,¹¹ M. Shao,³⁷ M. Sharma,²⁹ W. Q. Shen,³⁸ S. S. Shimanskiy,¹¹ E. Sichtermann,²¹ F. Simon,²² R. N. Singaraju,⁴⁴ N. Smirnov,⁴⁹ R. Snellings,²⁷ G. Sood,⁴³ P. Sorensen,³ J. Sowinski,¹⁶ J. Speltz,¹⁷ H. M. Spinka,¹ B. Srivastava,³² A. Stadnik,¹¹ T. D. S. Stanislaus,⁴³ R. Stock,¹³ A. Stolpovsky,⁴⁷ M. Strikhanov,²⁵ B. Stringfellow,³² A. A. P. Suaide,³⁶ E. Sugarbaker,²⁸ M. Sumner,¹⁰ Z. Sun,²⁰ B. Surrow,²² M. Swanger,⁹ T. J. M. Symons,²¹ A. Szanto de Toledo,³⁶ A. Tai,⁷ J. Takahashi,³⁶ A. H. Tang,³ T. Tarnowsky,³² D. Thein,⁷ J. H. Thomas,²¹ A. R. Timmins,² S. Timoshenko,²⁵ M. Tokarev,¹¹ S. Trentalange,⁷ R. E. Tribble,⁴⁰ O. D. Tsai,⁷ J. Ulery,³² T. Ullrich,³ D. G. Underwood,¹ G. Van Buren,³ N. van der Kolk,²⁷ M. van Leeuwen,²¹ A. M. Vander Molen,²⁴ R. Varma,¹⁵ I. M. Vasilevski,¹² A. N. Vasiliev,³¹ R. Vernet,¹⁷ S. E. Vigdor,¹⁶ Y. P. Viyogi,⁴⁴ S. Vokal,¹¹ S. A. Voloshin,⁴⁷ W. T. Waggoner,⁹ F. Wang,³² G. Wang,¹⁹ J. S. Wang,²⁰ X. L. Wang,³⁷ Y. Wang,⁴² J. W. Watson,¹⁹ J. C. Webb,¹⁶ G. D. Westfall,²⁴ A. Wetzler,²¹ C. Whitten, Jr.,⁷ H. Wieman,²¹ S. W. Wissink,¹⁶ R. Witt,⁴⁹ J. Wood,⁷ J. Wu,³⁷ N. Xu,²¹ Q. H. Xu,²¹ Z. Xu,³ P. Yepes,³⁵ I-K. Yoo,³³ V. I. Yurevich,¹¹ W. Zhan,²⁰ H. Zhang,³ W. M. Zhang,¹⁹ Y. Zhang,³⁷ Z. P. Zhang,³⁷ Y. Zhao,³⁷ C. Zhong,³⁸ R. Zoulkarneev,¹² Y. Zoulkarneeva,¹² A. N. Zubarev,¹¹ and J. X. Zuo³⁸

(STAR Collaboration)

- ¹Argonne National Laboratory, Argonne, Illinois 60439, USA
- ²University of Birmingham, Birmingham, United Kingdom
- ³Brookhaven National Laboratory, Upton, New York 11973, USA
- ⁴California Institute of Technology, Pasadena, California 91125, USA
- ⁵University of California, Berkeley, California 94720, USA
- ⁶University of California, Davis, California 95616, USA
- ⁷University of California, Los Angeles, California 90095, USA
- ⁸Carnegie Mellon University, Pittsburgh, Pennsylvania 15213, USA
- ⁹Creighton University, Omaha, Nebraska 68178, USA
- ¹⁰Nuclear Physics Institute AS CR, 250 68 Řež/Prague, Czech Republic
- ¹¹Laboratory for High Energy (JINR), Dubna, Russia
- ¹²Particle Physics Laboratory (JINR), Dubna, Russia
- ¹³University of Frankfurt, Frankfurt, Germany
- ¹⁴Institute of Physics, Bhubaneswar 751005, India
- ¹⁵Indian Institute of Technology, Mumbai, India
- ¹⁶Indiana University, Bloomington, Indiana 47408, USA
- ¹⁷Institut de Recherches Subatomiques, Strasbourg, France
- ¹⁸University of Jammu, Jammu 180001, India
- ¹⁹Kent State University, Kent, Ohio 44242, USA
- ²⁰Institute of Modern Physics, Lanzhou, China
- ²¹Lawrence Berkeley National Laboratory, Berkeley, California 94720, USA
- ²²Massachusetts Institute of Technology, Cambridge, Massachusetts 02139-4307, USA
- ²³Max-Planck-Institut für Physik, Munich, Germany
- ²⁴Michigan State University, East Lansing, Michigan 48824, USA
- ²⁵Moscow Engineering Physics Institute, Moscow Russia
- ²⁶City College of New York, New York, New York 10031, USA
- ²⁷NIKHEF and Utrecht University, Amsterdam, The Netherlands
- ²⁸The Ohio State University, Columbus, Ohio 43210, USA
- ²⁹Panjab University, Chandigarh 160014, India
- ³⁰Pennsylvania State University, University Park, Pennsylvania 16802, USA
- ³¹Institute of High Energy Physics, Protvino, Russia
- ³²Purdue University, West Lafayette, Indiana 47907, USA
- ³³Pusan National University, Pusan, Republic of Korea
- ³⁴University of Rajasthan, Jaipur 302004, India
- ³⁵Rice University, Houston, Texas 77251, USA
- ³⁶Universidade de Sao Paulo, Sao Paulo, Brazil
- ³⁷University of Science & Technology of China, Hefei 230026, China
- ³⁸Shanghai Institute of Applied Physics, Shanghai 201800, China
- ³⁹SUBATECH, Nantes, France
- ⁴⁰Texas A&M University, College Station, Texas 77843, USA
- ⁴¹University of Texas, Austin, Texas 78712, USA
- ⁴²Tsinghua University, Beijing 100084, China
- ⁴³Valparaiso University, Valparaiso, Indiana 46383, USA
- ⁴⁴Variable Energy Cyclotron Centre, Kolkata 700064, India
- ⁴⁵Warsaw University of Technology, Warsaw, Poland
- ⁴⁶University of Washington, Seattle, Washington 98195, USA
- ⁴⁷Wayne State University, Detroit, Michigan 48201, USA
- ⁴⁸Institute of Particle Physics, CCNU (HZNU), Wuhan 430079, China
- ⁴⁹Yale University, New Haven, Connecticut 06520, USA
- ⁵⁰University of Zagreb, Zagreb, HR-10002, Croatia

(Received 28 April 2006; published 16 October 2006)

The STAR Collaboration at the Relativistic Heavy Ion Collider reports measurements of azimuthal correlations of high transverse momentum (p_T) charged hadrons in Au + Au collisions at higher p_T than reported previously. As p_T is increased, a narrow, back-to-back peak emerges above the decreasing background, providing a clear dijet signal for all collision centralities studied. Using these correlations, we perform a systematic study of dijet production and suppression in nuclear collisions, providing new constraints on the mechanisms underlying partonic energy loss in dense matter.

Nuclear collisions at high energy may produce conditions sufficient for the formation of a deconfined plasma of quarks and gluons [1]. The high-density QCD matter [1,2] generated in these collisions can be probed via propagation of hard scattered partons, which have been predicted to lose energy in the medium primarily through gluon bremsstrahlung [3–6]. The medium alters the fragmentation of the parent partons, providing experimental observables that are sensitive to the properties of QCD matter at high density.

The study of high transverse momentum (p_T) hadron production in heavy ion collisions at the Relativistic Heavy Ion Collider (RHIC) has yielded several novel results [7], including the strong suppression relative to $p + p$ collisions of both inclusive hadron yields [8–11] and back-to-back azimuthal (ϕ) correlations [12]. Azimuthal correlations of high p_T hadrons reflect the fragmentation of outgoing partons produced dominantly in $2 \rightarrow 2$ hard scattering processes (“dijets” [13]). The back-to-back correlation strength has shown sensitivity to the in-medium path length of the parton [14], while the distribution of low p_T hadrons recoiling from a high p_T particle is broadened azimuthally and softened in central collisions [15], qualitatively consistent with dissipation of jet energy to the medium. However, those correlation measurements required large background subtraction, and quantitative study of the properties of the away-side jet has been limited. Previous correlation measurements also were constrained to a p_T region in which the hadron flavor content and baryon fraction exhibit substantial differences from jet fragmentation in elementary collisions [16–18].

In this Letter, we present measurements of azimuthal correlations of charged hadrons in Au + Au collisions at $\sqrt{s_{NN}} = 200$ GeV over a much broader transverse momentum range than previously reported. The p_T range extends to the region where previous studies suggest that particle production is dominated by jet fragmentation [16–18]. Increasing p_T reduces the combinatoric background and, for all centralities, reveals narrow back-to-back peaks indicative of dijets. A quantitative study of the centrality and p_T dependence of dijet fragmentation may provide new constraints on partonic energy loss and properties of the dense medium (e.g., [19]).

The measurements were carried out with the STAR experiment [20], which is well-suited for azimuthal correlation studies due to the full azimuthal (2π) coverage of its time projection chamber. This analysis is based on 30×10^6 minimum-bias and 18×10^6 central Au + Au collisions at $\sqrt{s_{NN}} = 200$ GeV, combining the 2001 data set with the high statistics data set collected during the 2004 run. 10×10^6 $d + Au$ events collected in 2003 are also included in the analysis. Event and track selection are similar to previous STAR high p_T studies [10,21]. This

analysis used charged tracks from the primary vertex with pseudorapidity $|\eta| < 1.0$.

As in our original studies of high p_T azimuthal correlations [12], transverse momentum-ordered jetlike correlations are measured by selecting high p_T trigger particles and studying the azimuthal distribution of associated particles ($p_T^{\text{assoc}} < p_T^{\text{trig}}$) relative to the trigger particle above a threshold p_T . The trigger-associated technique facilitates jet studies in the high-multiplicity environment of a heavy ion collision, where full jet reconstruction using standard methods is difficult. A particle may contribute to more than one hadron pair in an event, both as trigger and as associated particle, though for the high p_T ranges considered here, the rate of contribution to multiple pairs is small. The pair yield is corrected for associated particle tracking efficiency, with an uncertainty of 5% that is highly correlated over the momentum range considered here. The effect of momentum resolution on the pair yield is estimated to be less than 1%, and no correction for it was applied. A correction was also applied for nonuniform azimuthal acceptance, but not for the effects of the single-track cut $|\eta| < 1.0$. The single-track acceptance is independent of p_T and uniform on η for $p_T > 3$ GeV/c and $|\eta| < 1$. The near-side ($\Delta\phi \sim 0$) correlated yield at large $|\Delta\eta|$ is negligible.

Figure 1 shows dihadron azimuthal distributions normalized per trigger particle for central (0%–5%) Au + Au collisions. p_T^{trig} increases from left to right, and two p_T^{assoc} ranges are shown. The height of the background away from the near- ($\Delta\phi \sim 0$) and away-side ($|\Delta\phi| \sim \pi$) peaks, which is related to the inclusive yield, is similar

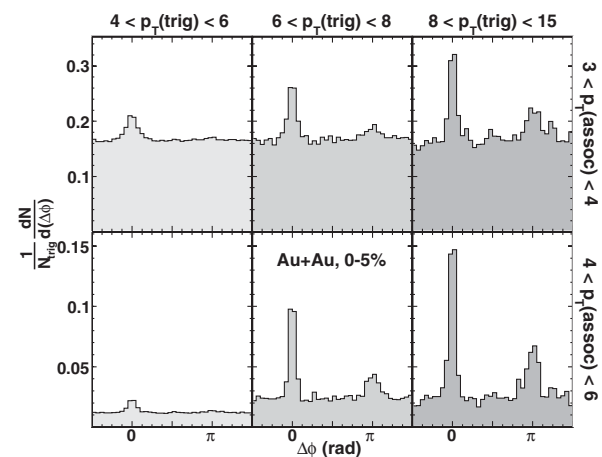


FIG. 1. Azimuthal correlation histograms of high p_T charged hadron pairs for 0%–5% Au + Au events, for various p_T^{trig} and p_T^{assoc} ranges. In the lower left panel, the yield is suppressed due to the constraint $p_T^{\text{assoc}} < p_T^{\text{trig}}$. All p_T values in this and succeeding figures have units GeV/c.

for different p_T^{trig} in each p_T^{assoc} interval. The background level decreases rapidly as p_T^{assoc} is raised, e.g., by an order of magnitude between the two rows in Fig. 1.

Near-side peaks are seen in all panels and indicate larger yields for higher p_T^{trig} at fixed p_T^{assoc} . Such an increase in the correlated yield is expected if the correlation is dominated by jet fragmentation, with higher p_T^{trig} biasing towards higher E_T jets. An away-side peak is not apparent at the lowest p_T^{trig} , consistent with previous studies of $\Delta\phi$ correlations in central Au + Au collisions in similar p_T^{trig} and p_T^{assoc} ranges [12]. However, an away-side peak emerges clearly above the background as p_T^{trig} is increased. The narrow, back-to-back peaks are indicative of the azimuthally back-to-back nature of dijets observed in elementary collisions.

Figure 2 shows the $\Delta\phi$ distributions for the highest p_T^{trig} range in Fig. 1 ($8 < p_T^{\text{trig}} < 15$ GeV/c) for midcentral (20%–40%) and central Au + Au collisions, as well as for $d + \text{Au}$ collisions. p_T^{assoc} increases from top to bottom; for the highest p_T^{assoc} (lower panels), the combinatorial background is negligible. We observe narrow correlation peaks in all p_T^{assoc} ranges. For each p_T^{assoc} , the near-side peak shows similar correlation strength above background for the three systems, while the away-side correlation strength decreases from $d + \text{Au}$ to central Au + Au. For $8 < p_T^{\text{trig}} < 15$ GeV/c and $p_T^{\text{assoc}} > 6$ GeV/c, a Gaussian fit to the away-side peak finds a width of $\sigma_{\Delta\phi} = 0.24 \pm 0.07$ for $d + \text{Au}$ and 0.20 ± 0.02 and 0.22 ± 0.02 for 20%–40% and 0%–5% Au + Au collisions, respectively.

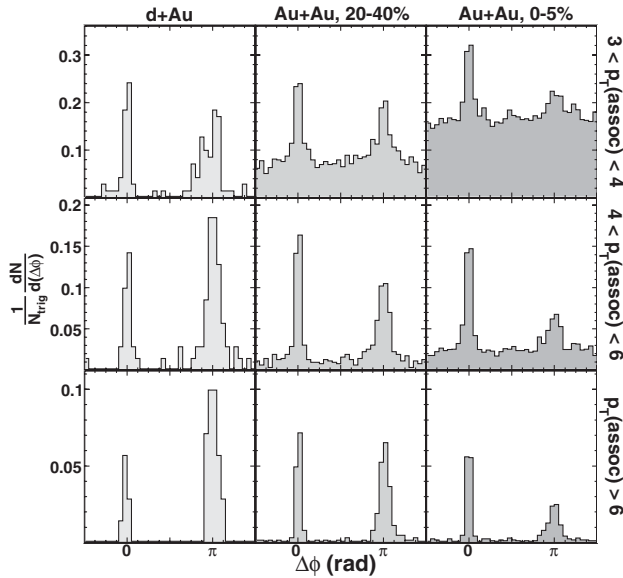


FIG. 2. Azimuthal correlation histograms of high p_T charged hadrons for $8 < p_T^{\text{trig}} < 15$ GeV/c, for $d + \text{Au}$, 20%–40% Au + Au, and 0%–5% Au + Au events. p_T^{assoc} increases from top to bottom.

No significant dependence of the widths on system or centrality is observed.

To quantify the correlated near- and away-side yields, we integrate the area under the peaks (near-side $|\Delta\phi| < 0.63$; away-side $|\Delta\phi - \pi| < 0.63$) and subtract the non-jetlike background. In previous analyses at lower p_T , anisotropic (“elliptic”) flow contributed significantly to the measured two-particle correlation, leading to large uncertainties in the extraction of jetlike yields [14,15]. In this analysis, the background contribution due to elliptic flow is estimated using a function $B[1 + v_2\{p_T^{\text{assoc}}\}v_2\{p_T^{\text{trig}}\} \times \cos(2\Delta\phi)]$, where the v_2 are extracted from standard elliptic flow analysis [14] and B is fitted to the region between the peaks ($0.63 < |\Delta\phi| < 2.51$), and is appreciable only for the lowest p_T^{assoc} range in Fig. 2. The uncertainty in the magnitude of elliptic flow introduces a small systematic uncertainty less than 5% on the extracted associated yields (Fig. 3).

Figure 3 shows the centrality dependence of the near- and away-side yields for the p_T^{trig} and p_T^{assoc} ranges in Fig. 2. The leftmost points in each panel correspond to $d + \text{Au}$ collisions, which we assume provide the reference distribution for jet fragmentation in vacuum. The near-side yields (left panel) show little centrality dependence, while the away-side yields (right panel) decrease with increasing centrality. The away-side centrality dependence is similar to our previous studies of dihadron azimuthal correlations for lower p_T ranges [12]. Note that the yields in different p_T^{assoc} bins for a given centrality may exhibit correlations due to their common trigger population.

The effect of the medium on dijet fragmentation can be explored in more detail using the p_T distributions of near-

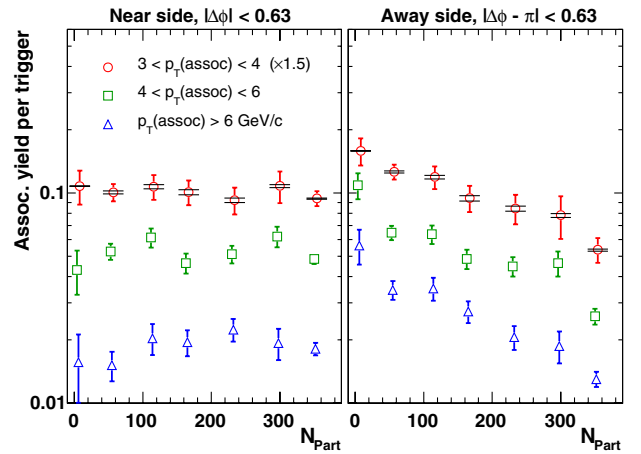


FIG. 3 (color online). Centrality dependence (number of participants N_{Part}) of near- and away-side yields in 200 GeV $d + \text{Au}$ (leftmost points) and Au + Au collisions, for $8 < p_T^{\text{trig}} < 15$ GeV/c and various p_T^{assoc} ranges. A semilog scale is used and data for $3 < p_T^{\text{assoc}} < 4$ GeV/c are scaled by 1.5 for clarity. The error bars are statistical. The horizontal bars for $3 < p_T^{\text{assoc}} < 4$ GeV/c show the systematic uncertainty due to background subtraction; it is negligible for higher p_T^{assoc} .

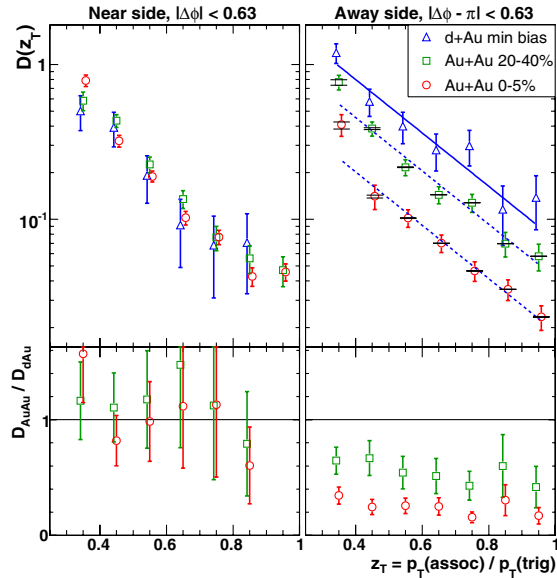


FIG. 4 (color online). Upper panels: $D(z_T)$ with $8 < p_T^{\text{trig}} < 15$ GeV/c, for near- (left) and away-side (right) correlations in $d + \text{Au}$ and $\text{Au} + \text{Au}$ collisions at $\sqrt{s_{NN}} = 200$ GeV. The dashed and solid lines are described in text. The horizontal bars on the away side show systematic uncertainty due to background subtraction. Lower panels: Ratio of $D(z_T)$ for $\text{Au} + \text{Au}$ relative to $d + \text{Au}$. The error bars are statistical in all panels.

and away-side associated hadrons. Figure 4 shows the trigger-normalized fragment distribution $D(z_T)$, where $z_T = p_T^{\text{assoc}}/p_T^{\text{trig}}$ [22]. $D(z_T)$ resembles a fragmentation function, though its shape in $p + p$ collisions is determined primarily by the partonic spectrum [23]. We investigate here its dependence on partonic energy loss. The z_T range in Fig. 4 corresponds to the p_T^{assoc} range for which dijets are observed above background (see Fig. 2). The near-side distributions (left panels) are similar over a broad range of z_T for all three systems, consistent with fragmentation in vacuum.

The similarity of the near-side fragmentation patterns could arise from small near-side energy loss due to a geometrical bias toward shorter in-medium path lengths (“surface bias”), as generated in several model calculations [24–27]. However, this similarity could also result from energy-independent energy loss generating a *partonic* energy distribution that is suppressed in $\text{Au} + \text{Au}$ but similar in shape to that in $p + p$ collisions, with the lost energy carried dominantly by low p_T hadrons. A leading-twist calculation of medium-modified dihadron fragmentation functions in similar p_T^{trig} and p_T^{assoc} intervals to those studied here [28] predicts a strong increase in the near-side associated yield for more central collisions, though no such increase is observed in Figs. 3 and 4.

The lower right panel in Fig. 4 shows the ratio of away-side $D(z_T)$ for 0%–5% and 20%–40% $\text{Au} + \text{Au}$ relative to $d + \text{Au}$. The ratio is approximately independent of z_T for

$z_T > 0.4$, with the yield suppressed by a factor 0.25 ± 0.06 for 0%–5% $\text{Au} + \text{Au}$ and 0.57 ± 0.06 for 20%–40% $\text{Au} + \text{Au}$ collisions. The away-side suppression for central collisions has a similar magnitude to that for inclusive spectra [10], though such a similarity is not expected *a priori* due to the different nature of the observable. A model calculation based on Baier-Dokshitzer-Mueller-Peigne-Schiff energy loss predicts a universal ratio between away-side and inclusive suppressions, with the away-side yield more suppressed [27].

The solid line in Fig. 4, upper right panel, is an exponential function fit to the $d + \text{Au}$ distribution (slope = -4.0 ± 0.6), with the dashed lines having the same exponential slope but magnitude scaled by factors 0.57 and 0.25. This illustrates the similarity in shape of $D(z_T)$ for different systems. As discussed for Fig. 2, the width of the away-side azimuthal distribution for high p_T pairs is also independent of centrality. To summarize our observations: Strong away-side high p_T hadron suppression is not accompanied by significant angular broadening or modification of the momentum distribution for $z_T > 0.4$.

A calculation incorporating partonic energy loss through modification of the fragmentation function [22] predicts the away-side trigger-normalized fragmentation function to be suppressed uniformly for $z_T > 0.4$ in central $\text{Au} + \text{Au}$ relative to $p + p$ collisions, in agreement with our measurement. However, the predicted magnitude of the suppression is ~ 0.4 , weaker than the measured value 0.25 ± 0.06 .

Energy loss in matter could be accompanied by away-side azimuthal broadening, due either to medium-induced acoplanarity of the parent parton [29] or to dominance of the away-side yield by medium-induced gluon radiation at a large angle. An opacity expansion calculation [30] predicts that the away-side yield for large energy loss is dominated by fragments of the induced radiation, with a strongly broadened azimuthal distribution up to $p_T \sim 10$ GeV/c. No azimuthal broadening of the away-side parent parton is predicted, though its fragments are obscured by the greater hadron yield from induced radiation. In contrast, we observe strong away-side suppression without large azimuthal broadening. However, measurements at $p_T^{\text{assoc}} < 1$ GeV/c do show an enhancement of the yield and significant azimuthal broadening of the away-side peak [15].

Large energy loss is thought to bias the jet population generating the high p_T *inclusive* hadron distribution towards jets produced near the surface and directed outward [24–27], which minimizes the path length in the medium. For back-to-back dihadrons, the total in-medium path length is minimized by a different geometric bias, towards jets produced near the surface but directed tangentially. A model calculation [31] incorporating quenching weights finds dihadron production dominated by such tangential pairs, with yield suppression consistent with our measure-

ments. Another calculation based on quenching weights, which explicitly takes into account the dynamical expansion of the medium [32], also reproduces the measured suppression but finds a significant contribution from non-tangential jet pairs, due to the finite probability to emit *zero* medium-induced gluons in finite path length [22,33] and to the rapid expansion and dilution of the medium. In this model, the relative contribution from the interior of the collision zone is larger for back-to-back dihadrons than for inclusive hadron production.

In summary, we have measured new fragmentation properties of jets and back-to-back dijets via high p_T hadron correlations in $\sqrt{s_{NN}} = 200$ GeV $d + Au$ and $Au + Au$ collisions. We observe the emergence at a suppressed rate of a narrow back-to-back dijet peak in central $Au + Au$ collisions, which may enable the first *differential* measurement of partonic energy loss. The observation at high p_T of strong suppression without modification of the away-side azimuthal and p_T^{assoc} distributions is in disagreement with several theoretical calculations. Other calculations reproduce aspects of these measurements but with somewhat different underlying mechanisms. New calculations are required to reconcile these differences and to clarify the physics underlying our observations. We expect that comparison of theory with the measurements reported here will provide new insights into both the nature of partonic energy loss and the properties of the medium generated in high energy nuclear collisions.

We thank the RHIC Operations Group and RCF at BNL and the NERSC Center at LBNL for their support. This work was supported in part by the HENP Divisions of the Office of Science of the U.S. DOE; the U.S. NSF; the BMBF of Germany; IN2P3, RA, RPL, and EMN of France; EPSRC of the United Kingdom; FAPESP of Brazil; the Russian Ministry of Science and Technology; the Ministry of Education and the NNSFC of China; IRP and GA of the Czech Republic; FOM of the Netherlands; DAE, DST, and CSIR of the Government of India; Swiss NSF; the Polish State Committee for Scientific Research; STAA of Slovakia; and the Korea Science and Engineering Foundation.

-
- [1] For recent theoretical reviews, see *Quark-Gluon Plasma. New Discoveries at RHIC: Case for the Strongly Interacting Quark-Gluon Plasma. Contributions from the RBRC Workshop held May 14–15, 2004*, edited by D. Rischke and G. Levin [Nucl. Phys. **A750**, 1 (2005)].
 - [2] I. Arsene *et al.* (BRAHMS Collaboration), Nucl. Phys. **A757**, 1 (2005); K. Adcox *et al.* (PHENIX Collaboration), Nucl. Phys. **A757**, 184 (2005); B. B. Back *et al.* (PHOBOS Collaboration), Nucl. Phys. **A757**, 28 (2005); J. Adams

- et al.* (STAR Collaboration), Nucl. Phys. **A757**, 102 (2005).
- [3] M. Gyulassy and X.N. Wang, Nucl. Phys. **B420**, 583 (1994).
- [4] R. Baier, D. Schiff, and B. G. Zakharov, Annu. Rev. Nucl. Part. Sci. **50**, 37 (2000).
- [5] M. Gyulassy *et al.*, in *Quark Gluon Plasma 3*, edited by R. C. Hwa and X.N. Wang (World Scientific, Singapore, 2004).
- [6] A. Kovner and U. A. Wiedemann, in *Quark Gluon Plasma 3*, edited by R. C. Hwa and X.N. Wang (World Scientific, Singapore, 2004).
- [7] P. Jacobs and X.N. Wang, Prog. Part. Nucl. Phys. **54**, 443 (2005).
- [8] K. Adcox *et al.* (PHENIX Collaboration), Phys. Rev. Lett. **88**, 022301 (2002).
- [9] C. Adler *et al.* (STAR Collaboration), Phys. Rev. Lett. **89**, 202301 (2002).
- [10] J. Adams *et al.* (STAR Collaboration), Phys. Rev. Lett. **91**, 172302 (2003).
- [11] B. B. Back *et al.* (PHOBOS Collaboration), Phys. Lett. B **578**, 297 (2004).
- [12] C. Adler *et al.* (STAR Collaboration), Phys. Rev. Lett. **90**, 082302 (2003).
- [13] L. DiLella, Annu. Rev. Nucl. Part. Sci. **35**, 107 (1985).
- [14] J. Adams *et al.* (STAR Collaboration), Phys. Rev. Lett. **93**, 252301 (2004).
- [15] J. Adams *et al.* (STAR Collaboration), Phys. Rev. Lett. **95**, 152301 (2005).
- [16] S. S. Adler *et al.* (PHENIX Collaboration), Phys. Rev. Lett. **91**, 172301 (2003).
- [17] J. Adams *et al.* (STAR Collaboration), Phys. Rev. Lett. **92**, 052302 (2004).
- [18] J. Adams *et al.* (STAR Collaboration), nucl-ex/0601042.
- [19] B. Müller and K. Rajagopal, Eur. Phys. J. C **43**, 15 (2005).
- [20] K. H. Ackermann *et al.*, Nucl. Instrum. Methods Phys. Res., Sect. A **499**, 624 (2003).
- [21] J. Adams *et al.* (STAR Collaboration), Phys. Rev. Lett. **91**, 072304 (2003).
- [22] X.N. Wang, Phys. Lett. B **595**, 165 (2004).
- [23] K. Adcox *et al.* (PHENIX Collaboration), hep-ex/0605039.
- [24] A. Drees, H. Feng, and J. Jia, Phys. Rev. C **71**, 034909 (2005).
- [25] A. Dainese, C. Loizides, and G. Paic, Eur. Phys. J. C **38**, 461 (2005).
- [26] K. J. Eskola *et al.*, Nucl. Phys. **A747**, 511 (2005).
- [27] B. Müller, Phys. Rev. C **67**, 061901(R) (2003).
- [28] A. Majumder, E. Wang, and X.N. Wang, nucl-th/0412061.
- [29] R. Baier *et al.*, Nucl. Phys. **B484**, 265 (1997).
- [30] I. Vitev, Phys. Lett. B **630**, 78 (2005).
- [31] A. Dainese, C. Loizides, and G. Paic, Acta Phys. Hung. A **27**, 245 (2006).
- [32] T. Renk, hep-ph/0602045.
- [33] C. A. Salgado and U. A. Wiedemann, Phys. Rev. Lett. **89**, 092303 (2002).